PHYSICAL REVIEW B **70**, 174512 (2004)

Interplay of superconductivity and structural phase transition in the clathrate Ba_6Ge_{25}

H. Q. Yuan,[1,2,*] F. M. Grosche,[1,3] W. Carrillo-Cabrera,[1] V. Pacheco,[1,†] G. Sparn,[1] M. Baenitz,[1]
U. Schwarz,[1] Yu. Grin,[1] and F. Steglich[1]
[1]*Max-Planck-Institute for Chemical Physics of Solids, Nöthnitzer Straße 40, 01187 Dresden, Germany*
[2]*Department of Physics, Xiangtan University, Xiangtan 411105, Hunan, People's Republic of China*
[3]*Department of Physics, Royal Holloway, University of London, Egham TW20 0EX, United Kingdom*
(Received 7 March 2004; revised manuscript received 25 August 2004; published 17 November 2004)

The cubic compound Ba_6Ge_{25} undergoes a structural phase transition around 200 K, below which the electrical resistivity increases abruptly. However, out of this "bad" metallic state ($\rho_0 \simeq 1.5\ \mathrm{m}\Omega\ \mathrm{cm}$), BCS-like superconductivity occurs at very low temperature ($T_c \approx 0.24$ K). By applying hydrostatic pressure, the structural phase transition is suppressed at $p_c \simeq 2.8$ GPa, but the superconducting transition temperature T_c increases remarkably, reaching a maximum of $T_c \simeq 3.8$ K at $p \sim p_c$. To understand these unusual properties, we have measured the upper critical magnetic field H_{c2} for Ba_6Ge_{25} and its isostructural compound $Na_2Ba_4Ge_{25}$ under pressure, from which the density of states at the Fermi energy $N(E_F)$ is determined. It demonstrates that, in Ba_6Ge_{25}, the structural phase transition causes a significant reduction of $N(E_F)$ (by a factor of about 4) and therefore largely weakens superconductivity. Furthermore, the drastic enhancement of T_c under pressure is found to be solely governed by $N(E_F)$.

DOI: 10.1103/PhysRevB.70.174512 PACS number(s): 74.25.Fy, 74.25.Jb, 74.62.Fj, 74.70.Wz

I. INTRODUCTION

In the last decade, there has been an increasing interest in the investigation of the group IV (Si, Ge, Sn) clathrates due to the discovery of superconductivity[1] and magnetism[2] in these compounds, and their potential applications as thermoelectric[3] and low-compressibility[4] materials.

Recently, a new type of superconducting clathrates, Ba_6Ge_{25} and $Na_2Ba_4Ge_{25}$, was reported.[5] Ba_6Ge_{25} belongs to the clathrate-IX structure type (Pearson symbol $cP124$).[6,7] It is characterized by a three-dimensional (3D) chiral framework of condensed Ge_{20} pentagonal dodecahedra (pdods) embedded in a 3D-channel labyrinth. Each Ge_{20} is centered by a Ba atom (Ba1) while the other Ba atoms (Ba2 and Ba3) occupy the cavities in the zeolite-like labyrinth created by the dense piling of pdods. There are two Ba1 and three Ba2 sites as well as one Ba3 site per formula unit. $Na_2Ba_4Ge_{25}$ is isostructural to Ba_6Ge_{25}, formed by randomly substituting $2/3$ of the Ba2 sites in Ba_6Ge_{25} with Na.[8] According to the Zintl–Klemm model, one can express Ba_6Ge_{25} as $(Ba^{2+})_6((3b)Ge^{1-})_8((4b)Ge^{0+})_{17}(4e^-)$ and $Na_2Ba_4Ge_{25}$ as $(Na^{1+})_2(Ba^{2+})_4((3b)Ge^{1-})_8((4b)Ge^{0+})_{17}(2e^-)$. This estimation gives four and two excess electrons per formula unit of Ba_6Ge_{25} and $Na_2Ba_4Ge_{25}$, respectively. Four formula units constitute a cubic cell with a lattice parameter of $a = 14.5564(2)$ Å for Ba_6Ge_{25} and of $a = 14.4703(2)$ Å for $Na_2Ba_4Ge_{25}$.

Ba_6Ge_{25} exhibits rich properties at low temperatures.[5,9] At ambient pressure, Ba_6Ge_{25} undergoes a two-step structural phase transition at temperatures of $T_{S1} \approx 215$ K and $T_{S2} \approx 180$ K due to the Ge–Ge bond breaking combined with the displacement of neighboring Ba atoms to the split positions.[10] The structural transition is accompanied by drastic changes of both transport and thermodynamic properties.[9] The magnetic susceptibility is negative over the whole temperature range and decreases steeply at the structural phase transition. Upon cooling down, the electrical resistivity $\rho(T)$ exhibits metallic behavior at high temperature, but increases abruptly at T_{S1} and subsequently again at T_{S2}. It slowly rises with further decreasing temperature and approaches a saturation value of $\rho_0 \simeq 1.5\ \mathrm{m}\Omega\ \mathrm{cm}$ below 10 K. Surprisingly, BCS-like superconductivity occurs at $T_c \simeq 0.24$ K out of the resulting bad metal.[5] Upon applying pressure, the structural phase transition is shifted to lower temperature while T_c increases drastically. T_c reaches a maximum value of $T_c \simeq 3.8$ K at a critical pressure of $p_c \simeq 2.8$ GPa, where the structural distortion is completely suppressed and the system displays metallic behavior above T_c, resembling the case of $Na_2Ba_4Ge_{25}$ at $p \geqslant 0$.[5]

To understand these fascinating phenomena observed in Ba_6Ge_{25}, here we analyze the possible reasons for the enhancement of T_c under pressure. For comparison, the pressure dependence of T_{S1}, T_{S2}, and T_c for Ba_6Ge_{25}, previously presented in Ref. 5, is replotted as a function of lattice parameter a in Fig. 1 together with that of $Na_2Ba_4Ge_{25}$. The relationship between pressure and lattice parameter for Ba_6Ge_{25} was obtained from high pressure x-ray diffraction experiments at ambient temperature employing a synchrotron source, which gives a volume bulk modulus of $B_0 = 44(2)$ GPa and its pressure derivative of $B_0' = 5.8(8)$. As an approximation, the same bulk modulus was also used for $Na_2Ba_4Ge_{25}$. Contrary to Ba_6Ge_{25}, $Na_2Ba_4Ge_{25}$ does not undergo a structural phase transition. From Fig. 1, one can see that the critical lattice parameter a_c of Ba_6Ge_{25} is much smaller than the ambient-pressure lattice parameter of $Na_2Ba_4Ge_{25}$, indicating that the occurrence of the structural phase transition is not simply governed by volume. In light of this, it is surprising to observe that T_c of these two compounds is equal at $a \approx 14.47$ Å, which is the ambient-pressure lattice parameter of $Na_2Ba_4Ge_{25}$. This coincidence seems more accidental rather than being due to a physical effect. As shown in Fig. 1, Ba_6Ge_{25} has a much lower T_c than

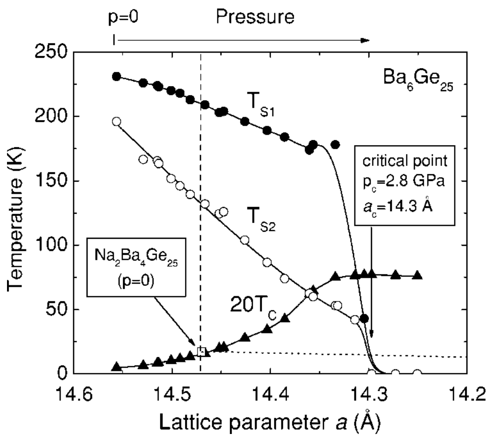

FIG. 1. The transition temperature vs lattice parameter (pressure) phase diagram for Ba_6Ge_{25}. For the calculation of the lattice parameters see text. The values of T_c are multiplied by a factor of 20. For a better comparison, $T_c(a)$ of $Na_2Ba_4Ge_{25}$ (□) at ambient pressure is marked by a vertical dashed line, while the dependence of T_c on the lattice parameter a is represented by the dotted line.

$Na_2Ba_4Ge_{25}$ at ambient pressure. In Ba_6Ge_{25}, the specific heat and magnetic susceptibility give a bulk superconducting transition at $T_c \simeq 0.14$ K and the resistivity shows $T_c \simeq 0.24$ K. By comparison, $Na_2Ba_4Ge_{25}$ demonstrates a much higher T_c (~ 0.84 K) from both specific heat and resistivity at ambient pressure. Correspondingly, a higher Sommerfeld coefficient γ is obtained in $Na_2Ba_4Ge_{25}$ ($\simeq 33.3$ mJ/mol K^2) than in Ba_6Ge_{25} ($\simeq 21.5$ mJ/mol K^2), revealing that the electronic density of states $N(E_F)$ in $Na_2Ba_4Ge_{25}$ is higher than in Ba_6Ge_{25}. On the other hand, once the structural transition (T_{S1}, T_{S2} in Fig. 1) of Ba_6Ge_{25} is suppressed by applying pressure, these two compounds behave very similarly both in the superconducting and in the normal state. However, Ba_6Ge_{25} now shows a much higher T_c than $Na_2Ba_4Ge_{25}$. The relatively larger T_c in Ba_6Ge_{25} at elevated pressure may be understood as follows: (1) Ba_6Ge_{25} has a nominally higher charge-carrier concentration than $Na_2Ba_4Ge_{25}$ and (2) Ba may have a stronger hybridization with the Ge states than Na as discussed for the type-I clathrates.[11] All these effects may enhance the density of states $N(E_F)$ and give rise to a higher T_c in Ba_6Ge_{25}.

In Fig. 2, T_c of Ba_6Ge_{25} is plotted as a function of the residual resistivity ρ_0. Remarkably, T_c can be nicely fitted by an exponential decrease of $T_c = 7.5\text{ K}\, e^{-2(\text{m}\Omega\text{cm})^{-1}\rho_0}$ (solid line in Fig. 2). According to the BCS formula,

$$T_c \propto \Theta_D \exp[-1/N(E_F)V], \qquad (1)$$

where Θ_D is the Debye temperature and V is the pairing potential arising from the electron-phonon interaction. Comparing Eq. (1) to the fitting function shown in Fig. 2, one finds that $\rho_0 \sim 1/N(E_F)$ if V and Θ_D are independent of pressure. This latter assumption is corroborated by the pressure dependence of T_c for $Na_2Ba_4Ge_{25}$. In Ba_6Ge_{25}, the residual resistivity ρ_0 strongly decreases with increasing pressure, suggesting a corresponding increase of $N(E_F)$. It is noted that the strong decrease of the residual resistivity ρ_0 under pressure is not due to effects like, e.g., grain-boundary scattering in the polycrystalline samples because applying pressure hardly changes the electrical resistivity at room temperature.[5]

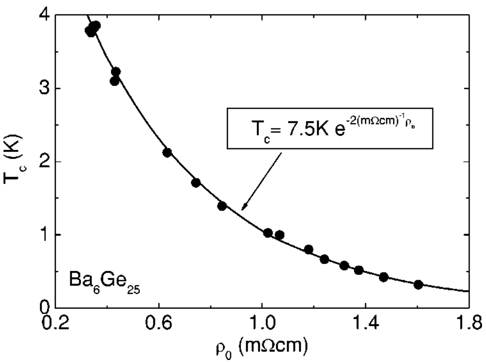

FIG. 2. T_c vs the residual resistivity ρ_0 for Ba_6Ge_{25}. The solid line is an exponential fit to the data points.

From the above discussion, one can see that the variation of $N(E_F)$ as a function of pressure may govern the stability of superconductivity in Ba_6Ge_{25}. The disorder resulting from the structural transition may smear out the density of states at the Fermi energy, which causes a significant reduction of $N(E_F)$. Recently, electronic band-structure calculations for Ba_6Ge_{25} and $Na_2Ba_4Ge_{25}$, using the linear muffin-tin orbital method within the local-density approximation,[12] have shown that the barium states strongly contribute to $N(E_F)$. A sharp peak in the density of states is found close to the Fermi level in the ideal Ba_6Ge_{25} (i.e., all the Ba atoms are at their average positions), but this peak is split while shifting the Ba2 atoms towards one of the split positions. The reduction of $N(E_F)$ may also explain the structural-transition induced anomalies on the thermodynamic properties such as the magnetic susceptibility. To provide experimental evidence in support of these speculations, in this paper we study the upper critical field of Ba_6Ge_{25} and $Na_2Ba_4Ge_{25}$ under hydrostatic pressure, from which the pressure dependence of the density of states $N(E_F)$ is inferred. It demonstrates that $N(E_F)$ of Ba_6Ge_{25} plays a governing role for the enhancement of T_c under pressure, increasing by a factor of about 4 as the structural distortion is suppressed.

II. EXPERIMENTAL METHODS

Polycrystalline samples of Ba_6Ge_{25} and $Na_2Ba_4Ge_{25}$ have been prepared by a high frequency melting technique in an argon protective atmosphere.[9] Powder x-ray diffraction and metallography identify them as being single phase. It is noted that the samples measured here are not the same as those studied before in Ref. 5. Since the density of states at the Fermi energy is simply proportional to the Sommerfeld coefficient γ, measurements of heat capacity under pressure may provide direct information about $N(E_F)$. However, Ba_6Ge_{25} has a small volume specific heat, which prevents it from being resolved in the experiments using a standard piston-cylinder pressure cell. Therefore, we have chosen an alternative approach to estimate $N(E_F)$, namely by measuring the upper critical magnetic field of the superconductor (H_{c2}).

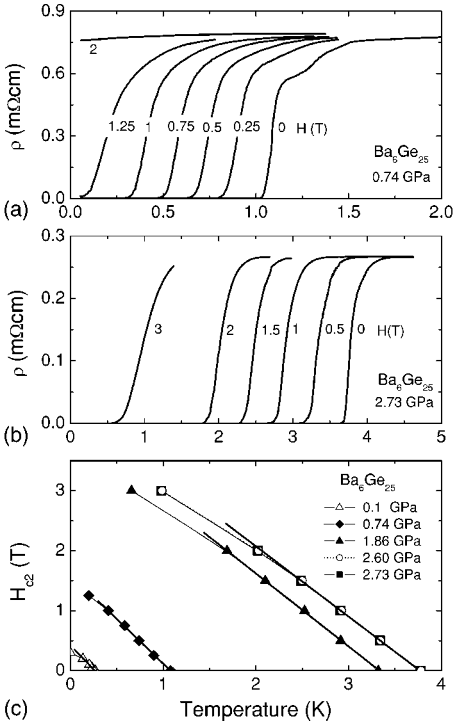

FIG. 3. The temperature dependence of the electrical resistivity $\rho(T)$ for Ba_6Ge_{25} at various magnetic fields: (a) $p=0.74$ GPa and (b) $p=2.73$ GPa. (c) The upper critical field $H_{c2}(T)$ for $p=0.1, 0.74, 1.86, 2.6$, and 2.73 GPa. When the applied field exceeds $H_{c2}(T)$, the entire specimen reverts to the normal state. The thick lines illustrate the linear fits to the data near T_c.

The electrical resistivity $\rho(T)$ has been measured by using a low power AC four-terminal method in a dilution refrigerator. To reach high pressure, we employ a CuBe/MP35N nonmagnetic hydrostatic clamp cell filled with a 1:1 mixture of iso-pentane and *n*-pentane as pressure transmitting medium. The relatively large volume of this cell allows simultaneous measurements on multiple samples up to 3 GPa, which offers an opportunity to study the two different compounds under the same conditions. The pressure was determined within an error of 0.05 GPa at low temperature from the superconducting transition temperature of Sn. Absolute resistivity values for the small crystals were obtained by extrapolating the high pressure, room temperature data to zero pressure to match the ambient pressure, room temperature resistivity measured on large reference crystals.

III. RESULTS AND DISCUSSION

In Fig. 3, we present the results of the upper critical magnetic field for Ba_6Ge_{25}. As an example, the temperature dependence of the resistivity $\rho(T)$ for $p=0.74$ GPa and 2.73 GPa at various magnetic fields is shown in Figs. 3(a) and 3(b), respectively. The broad superconducting transition at low pressures might be due to sample inhomogeneities. One can see that the superconducting transitions are rapidly suppressed by applying a magnetic field. In Fig. 3(c), the critical field H_{c2} is plotted as a function of temperature for various pressures. The thick lines represent the linear fits for the data near T_c. One can see that all the thick lines are nearly parallel, indicating a weak pressure dependence of the initial slope of the upper critical field. Similar behavior of H_{c2} is also observed in $Na_2Ba_4Ge_{25}$.

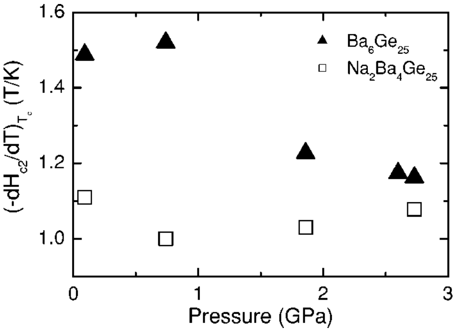

FIG. 4. Values of the initial slope H'_{c2} vs pressure for Ba_6Ge_{25} (▲) and $Na_2Ba_4Ge_{25}$ (□).

The values of the initial slope of the upper critical field $H'_{c2}=(-dH_{c2}/dT)_{Tc}$ are shown in Fig. 4 for Ba_6Ge_{25} and $Na_2Ba_4Ge_{25}$. Evidently, H'_{c2} of $Na_2Ba_4Ge_{25}$ is nearly pressure independent between 1 and 3 GPa. By applying pressure to suppress the structural distortion in Ba_6Ge_{25}, T_c undergoes a drastic enhancement. However, no significant change of H'_{c2} is observed in Ba_6Ge_{25} under pressure. We note that the sample of Ba_6Ge_{25} studied here exhibits a relatively small value of $H'_{c2}\simeq 1.5$ T/K at $p=0.1$ GPa in comparison with the previous results measured at ambient pressure ($H'_{c2}\simeq 2.9$ T/K).[5] Since in polycrystalline samples the grain boundaries and the grain geometries may affect the critical current and the penetration depth, respectively, the difference in the absolute values of H'_{c2} might be mainly due to the different grain geometries in the two samples measured.

Based on the evaluation of the Ginzburg-Landau parameters from the BCS-Gorkov equations, a few superconducting and normal-state parameters can be estimated from the measurements of the upper critical magnetic field.[13,14] Within the BCS theory, the initial slope of the upper critical field can be expressed by

$$\begin{aligned} H'_{c2} &= -\left.\frac{dH_{c2}}{dT}\right|_{T_c} \\ &= R(\lambda_{tr})\left[\left(1.18\times 10^{35}\frac{\mathrm{T\,m^2\,K^2}}{\mathrm{J^2}}\right)\frac{\gamma^2 T_c}{S^2} \right.\\ &\qquad \left. + \left(4490\frac{\mathrm{T\,m^2\,K}}{\Omega \mathrm{J}}\right)\gamma\rho_0\right]. \end{aligned} \tag{2}$$

Here S is the Fermi surface area on which the Cooper pairs are formed; $R(\lambda_{tr})$ varies monotonously between $R(0)=1$ in the dirty limit and $R(\infty)=1.17$ in the clean limit. In the dirty limit, the second term in Eq. (2) dominates and H'_{c2} can be written as[13]

$$H'_{c2}(\mathrm{dirty}) = \left(4490\frac{\mathrm{T\,m^2\,K^2}}{\Omega \mathrm{J}}\right)\gamma\rho_0. \tag{3}$$

Then γ can be estimated from the measurements of ρ_0 and H'_{c2} according to Eq. (3).

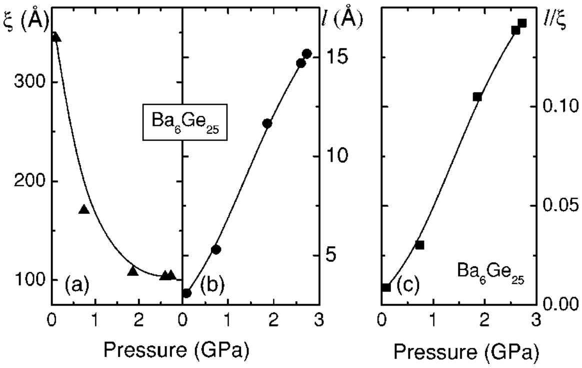

FIG. 5. The pressure dependence of the coherence length ξ (a), the mean-free path l (b), and the ratio l/ξ (c) for Ba_6Ge_{25}. The relation of $l/\xi \ll 1$ indicates that Ba_6Ge_{25} is in the dirty limit even at high pressures.

The electronic density of states $N(E_F)$ per formula unit can be calculated from

$$\gamma = \frac{\pi^2 k_B^2}{3}\frac{N(E_F)}{V_0}, \tag{4}$$

where V_0 is the cell volume per formula unit.

At ambient pressure, it has been demonstrated that Ba_6Ge_{25} is a bad metal with a very short mean-free path ($l \sim 3$ Å).[5] In order to confirm the feasibility of adopting the dirty limit in Ba_6Ge_{25} and $Na_2Ba_4Ge_{25}$ under pressure, we first examine the Ginzburg-Landau coherence length ξ as compared with the electronic mean-free path l, which are given by[5]

$$\xi^2 = 4.76 \times 10^4 (\text{T Å}^2)[H'_{c2}(\text{T/K}) \cdot T_c(\text{K})]^{-1} \tag{5}$$

and

$$l = 1200[k_F^2(\text{Å}^{-2}) \cdot \rho_0(\mu\Omega\ \text{cm})]^{-1}(\text{Å}). \tag{6}$$

Here, k_F is the wave vector at the Fermi surface. It is estimated here by assuming a spherical Fermi surface as for free electrons, which can be written as

$$k_F = (3\pi^2 n)^{1/3}, \tag{7}$$

where n is the electron density. The Hall-effect measurements showed that the charge-carrier concentration of Ba_6Ge_{25} at low temperature is close to the nominal value derived from the Zintl rule, and in the case of $Na_2Ba_4Ge_{25}$ the experiment gives a higher electron concentration.[9] For simplicity, we take the nominal value of n to estimate k_F here, which gives $k_F = 0.54(\text{Å})^{-1}$ for Ba_6Ge_{25} and 0.43 Å^{-1} for $Na_2Ba_4Ge_{25}$. Under hydrostatic pressure, we assume that it remains constant.

Figures 5 and 6 present the pressure dependences of the mean free path l, the coherence length ξ, and its ratio l/ξ for Ba_6Ge_{25} and $Na_2Ba_4Ge_{25}$, respectively. Both compounds exhibit $l \ll \xi$ at all pressures [see Fig. 5(c) and Fig. 6(c)], suggesting that the samples are in the dirty limit and one can employ Eq. (3) to calculate γ from ρ_0 and H'_{c2}. The corresponding density of states $N(E_F)$ can then be calculated from Eq. (4). Comparing Fig. 5 with Fig. 6, one can see that the compounds Ba_6Ge_{25} and $Na_2Ba_4Ge_{25}$ display an opposite pressure dependence of l and ξ. This distinct behavior may originate from the structural transition in Ba_6Ge_{25}. When the structural transition vanishes at $p_c \sim 2.7$ GPa, the mean-free path of Ba_6Ge_{25} approaches that of $Na_2Ba_4Ge_{25}$.

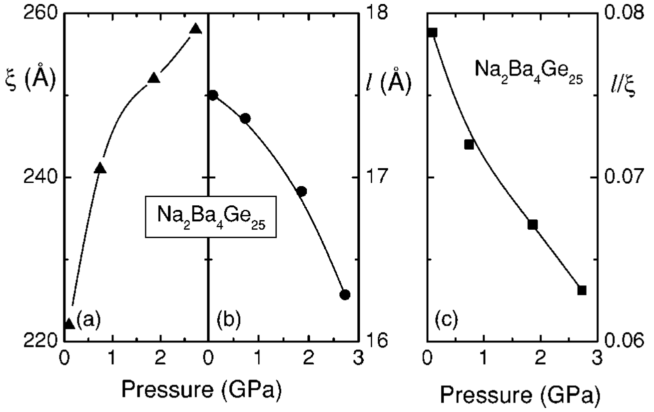

FIG. 6. The pressure dependence of the coherence length ξ (a), the mean-free path l (b), and the ratio l/ξ (c) for $Na_2Ba_4Ge_{25}$. The relation of $l/\xi \ll l$ indicates that $Na_2Ba_4Ge_{25}$ is in the dirty limit.

In Fig. 7, the pressure dependence of the obtained density of states $N(E_F)$ is shown for Ba_6Ge_{25} and $Na_2Ba_4Ge_{25}$. As expected from the analysis previously made in the Introduction, $N(E_F)$ of Ba_6Ge_{25} is strongly enhanced under pressure, increasing by a factor of about 4 at $p \sim p_c$. For the undistorted Ba_6Ge_{25}, $N(E_F, p)$ seems to saturate, which is again similar to the case of $Na_2Ba_4Ge_{25}$ but with a larger value.

It has been argued before that the density of states $N(E_F)$ might be closely associated with the residual resistivity ρ_0 in Ba_6Ge_{25} from the analysis of T_c and ρ_0. In Fig. 8(a), we plot ρ_0 against the experimentally obtained $1/N(E_F)$ for Ba_6Ge_{25}. It shows that all the data points fall on a straight line, confirming that $\rho_0 \sim 1/N(E_F)$ in the distorted Ba_6Ge_{25}. This is similar to the case of the widely studied A15 compounds (see, e.g., Ref. 15). Figure 8(b) shows T_c versus $1/N(E_F)$ for Ba_6Ge_{25}, which can be fitted by an exponential decay [T_c

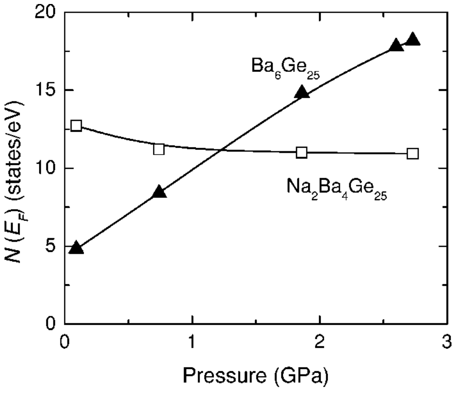

FIG. 7. The pressure dependence of the density of states $N(E_F)$ for Ba_6Ge_{25} (▲) and $Na_2Ba_4Ge_{25}$ (□). $N(E_F)$ of Ba_6Ge_{25} is enhanced by a factor of about 4 as its structural transition is suppressed at $p_c \sim 2.7$ GPa, whereas $Na_2Ba_4Ge_{25}$ shows a weak decrease of $N(E_F)$ under pressure.

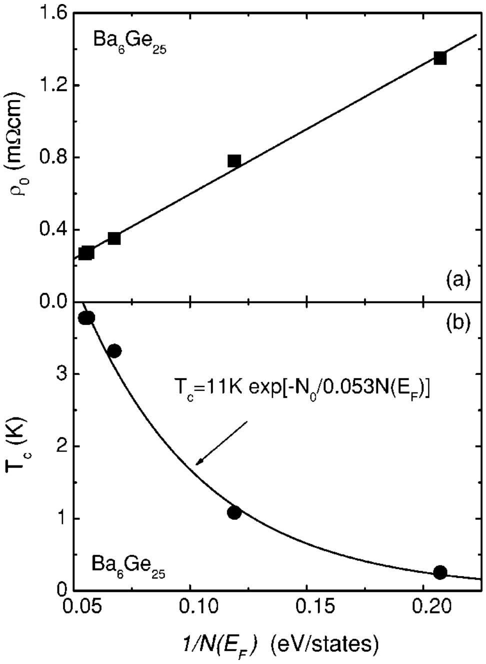

FIG. 8. The residual resistivity ρ_0 (a) and the superconducting transition temperature T_c (b) vs $1/N(E_F)$ for Ba_6Ge_{25}, which shows $\rho_0 \sim 1/N(E_F)$ and $T_c = 11$ K $\exp(-N_0/0.053N(E_F))$ where $N_0 = 1$ state/eV.

$= 11$ K $\exp(-N_0/0.053N(E_F))]$ where $N_0 = 1$ state/eV. All these results suggest that the density of states at the Fermi energy $N(E_F)$ governs the drastic enhancement of T_c under pressure in Ba_6Ge_{25} and that the structural transition results in a large reduction of $N(E_F)$. Other factors have minor effect on the superconductivity of Ba_6Ge_{25}.

The inverse relationship of $\rho_0 \sim 1/N(E_F)$ can be qualitatively understood by considering a sharp structure in the density of states near E_F with a width ΔW. Actually, recent band-structure calculations have revealed a peak of $N(E_F)$ in Ba_6Ge_{25}.[12] Sharp structures at the Fermi level may effectively be broadened by the strong scattering present in the bad metals such as Ba_6Ge_{25}. It is argued[15] that $N(E)$ must be averaged over ΔE, which becomes important when the uncertainty in energy ΔE approaches ΔW. ΔE is related to the quasiparticle lifetime. According to the uncertainty principle, one has

$$\Delta E \Delta t = \Delta E \cdot l/v_F = \hbar, \tag{8}$$

where v_F refers to the Fermi velocity. In the dirty limit as observed in our compounds, l is quite small and hence ΔE becomes large. Therefore, the smearing of $N(E_F)$ becomes very important, leading to a significant decrease of $N(E_F)$. Since ΔE goes as $1/l$, it means $\Delta E \sim \rho_0$. If one assumes a constant number of states near E_F, i.e., $\Delta E \cdot N(E_F) =$ constant, then one has $\rho_0 \sim 1/N(E_F)$.

Measurements of the thermopower[9] and the optical reflectivity[16] at ambient pressure appear to contradict this interpretation, revealing that below the structural phase transition the effective mass of electrons increases by a factor of about 4, but the relaxation time remains constant. These results are incompatible with the superconducting properties, the reason of which is still unclear. One possibility may arise from the charge-carrier concentration $n(T)$. Very recently, single-crystal x-ray diffraction measurements suggest that the number of excess electrons is reduced by $1.8e^-$ per formula unit at the structural phase transition due to the modification of the Ge bonds.[10] In the initial analysis of the thermopower[9] and the optical reflectivity,[16] it was assumed that $n(T)$ decreases monotonically upon cooling down. The stepwise reduction of the charge-carrier concentration at the structural phase transition would now make the analysis of the thermopower[9] and the optical reflectivity[16] consistent with our results.

IV. CONCLUSION

The remarkable pressure dependences of the structural phase transition and superconductivity observed in Ba_6Ge_{25} are discussed in comparison with its isostructural variant $Na_2Ba_4Ge_{25}$. To understand the huge enhancement of T_c in Ba_6Ge_{25} when its structural distortion is prevented by pressure, we have investigated the pressure dependence of the density of states $N(E_F)$ by measuring the upper critical magnetic field. It is shown that both compounds are in the dirty limit even under pressure and that the slope of the upper critical field H'_{c2} hardly depends on pressure. In Ba_6Ge_{25} the density of states $N(E_F)$ increases with increasing pressure (by a factor of about 4 up to $p \sim p_c$), but $Na_2Ba_4Ge_{25}$ shows a slight decrease of $N(E_F)$ under pressure. Moreover, we found a relationship of $\rho_0 \sim 1/N(E_F)$ for Ba_6Ge_{25}. All these suggest that the structural phase transition in Ba_6Ge_{25}, caused by the breaking of some Ge–Ge bonds, results in a significant reduction of $N(E_F)$. The pressure dependence of T_c is found to be governed by $N(E_F)$, providing a physical picture to describe the unusual behavior observed in Ba_6Ge_{25}.

ACKNOWLEDGMENTS

The authors acknowledge the helpful discussions with J. Mydosh, S. Paschen, J. Sichelschmidt, S. Yamanaka, and I. Zerec.

---

*Present address: Department of Physics, University of Illinois at Urbana-Champaign, 1110 West Green Street, Urbana, Illinois 61801. Electronic address: yuan@mrl.uiuc.edu

†Present address: Instituto de Fisica, Universidad Autónoma de Puebla, Apdo. Postal J-48, Puebla 72570, México.

[1] H. Kawaji, H. O. Horie, S. Yamanaka, and M. Ishikawa, Phys. Rev. Lett. **74**, 1427 (1995).

[2] B. C. Sales, B. C. Chakoumakos, R. Jin, J. R. Thompson, and D. Mandrus, Phys. Rev. B **63**, 245113 (2001); S. Paschen, W. Carrillo-Cabrera, A. Bentien, V. H. Tran, M. Baenitz, Yu. Grin,

and F. Steglich, *ibid.* **64**, 214404 (2001).

[3] G. S. Nolas, G. A. Slack, and S. B Schujman, in *Semiconductors and Semimetals*, edited by T. M. Tritt (Academic, San Diego, 2001), Vol. 69, p. 255.

[4] A. San-Miguel, P. Kéghélian, X. Blase, P. Mélinon, A. Perez, J. P. Itié, A. Polian, E. Reny, C. Cros, and M. Pouchard, Phys. Rev. Lett. **83**, 5290 (1999).

[5] F. M. Grosche, H. Q. Yuan, W. Carrillo-Cabrera, S. Paschen, C. Langhammer, F. Kromer, G. Sparn, M. Baenitz, Yu. Grin, and F. Steglich, Phys. Rev. Lett. **87**, 247003 (2001); H. Q. Yuan, F. M. Grosche, W. Carrillo-Cabrera, S. Paschen, C. Langhammer, G. Sparn, M. Baenitz, Yu. Grin, and F. Steglich, High Press. Res. **22**, 147 (2002).

[6] W. Carrillo-Cabrera, J. Curda, H. G. von Schnering, S. Paschen, and Yu. Grin, Z. Kristallogr. - New Cryst. Struct. **215**, 207 (2000).

[7] H. Fukuoka, K. Iwai, S. Yamanaka, H. Abe, K. Yoza, and L. Häming, J. Solid State Chem. **151**, 117 (2000); S. J. Kim, S. Hu, C. Uher, T. Hogan, B. Huang, J. D. Corbett, and M. G. Kanatzidis, *ibid.* **153**, 321 (2000).

[8] W. Carrillo-Cabrera, J. Curda, K. Peters, S. Paschen, Yu. Grin, and H. G. von Schnering, Z. Kristallogr. - New Cryst. Struct. **216**, 183 (2001).

[9] S. Paschen, V. H. Tran, M. Baenitz, W. Carrillo-Cabrera, Yu. Grin, and F. Steglich, Phys. Rev. B **65**, 134435 (2002).

[10] W. Carrillo-Cabrera, H. Borrmann, S. Paschen, M. Baenitz, F. Steglich, and Yu. Grin (unpublished).

[11] S. Saito and A. Oshiyama, Phys. Rev. B **51**, 2628 (1995); K. Moriguchi, M. Yonemura, A. Shintani, and S. Yamanaka, *ibid.* **61**, 9859 (2000).

[12] I. Zerec, A. Yaresko, P. Thalmeier, and Yu. Grin, Phys. Rev. B **66**, 045115 (2002).

[13] T. P. Orlando, E. J. McNiff, Jr., S. Foner, and M. R. Beasley, Phys. Rev. B **19**, 4545 (1979).

[14] N. R. Werthamer, E. Helfand, and P. C. Hohenberg, Phys. Rev. **147**, 295 (1966).

[15] H. Wiesmann, M. Gurvitch, A. K. Ghosh, H. Lutz, O. F. Kammerer, and M. Strongin, Phys. Rev. B **17**, 122 (1978).

[16] J. Sichelschmidt, V. Voevodin, S. Paschen, W. Carrillo-Cabrera, Yu. Grin, and F. Steglich, Acta Phys. Pol. B **34**, 613 (2003).